Received: September 19, 2014 | Accepted: October 21, 2014 | Web Released: October 30, 2014 CL-140880

Nanoscale Identification of Extracellular Organic Substances at the Microbe–Mineral Interface by Scanning Transmission X-ray Microscopy

Satoshi Mitsunobu,*[1] Ming Zhu,[1] Yasuo Takeichi,[2,3] Takuji Ohigashi,[4] Hiroki Suga,[5] Hiroko Makita,[6] Masahiro Sakata,[1] Kanta Ono,[2,3] Kazuhiko Mase,[2,3] and Yoshio Takahashi[2,7]

[1]*Graduate Division of Nutritional and Environmental Sciences, University of Shizuoka, Yada, Suruga-ku, Shizuoka 422-8526*
[2]*Institute of Materials Structure Science, High-Energy Accelerator Research Organization (KEK), Oho, Tsukuba, Ibaraki 305-0801*
[3]*The Graduate University for Advanced Studies, 1-1 Oho, Tsukuba, Ibaraki 305-0801*
[4]*UVSOR Facility, Institute for Molecular Science, Myodaiji, Okazaki, Aichi 444-8585*
[5]*Department of Earth and Planetary Systems Science, Hiroshima University, Kagamiyama, Higashi-Hiroshima, Hiroshima 739-8526*
[6]*Japan Agency for Marine-Earth Science and Technology (JAMSTEC), Natsushima-cho, Yokosuka, Kanagawa 237-0061*
[7]*Department of Earth and Planetary Science, The University of Tokyo, Hongo, Bunkyo-ku, Tokyo 113-0033*

(E-mail: mitunobu@u-shizuoka-ken.ac.jp)

In the present study, we applied a scanning transmission X-ray microscopy (STXM) technique to investigate the spatial distribution of biomolecules at the microbe–mineral boundary during bioleaching process of pyrite (FeS_2). STXM-based carbon and oxygen near-edge X-ray absorption fine structure (NEXAFS) directly showed that polysaccharides were localized within 150 nm of the bacteria–pyrite boundary and that sessile bioleaching bacteria produced polysaccharides-abundant extracellular biomolecules on the pyrite grain. The STXM-based NEXAFS technique has multiple advantages: (i) a high spatial resolution less than 50 nm, (ii) a nondestructive analytical technique with a high element of specificity, (iii) X-ray spectroscopic chemical speciation useful for the analysis of hydrated biomolecules. Thus, the STXM-based NEXAFS technique is a powerful tool to investigate the mechanism of biological process occurring at the microbe–mineral interface.

Mineral leaching by bacteria has been used as a low-cost engineering technique for extracting metals (e.g., Fe and Cu) from metal sulfide ores such as pyrite (FeS_2) and chalcopyrite ($CuFeS_2$).[1] Bioleaching engineering has generally been operated under mesophilic conditions,[2] where the bacteria occur in biofilms on metal sulfides. Biofilms are interface-associated colonies of microbes embedded in a matrix of biopolymers. The biotic leaching rate of a metal sulfide is 30–40 times faster than abiotic leaching.[3,4] Previous studies implied that microbes produce some extracellular polymeric substances (EPS) to enhance access to the mineral surface and dissolution of the mineral.[1,5–7] However, little is known about the biochemical process at the mineral–bacteria interface, because the scale of the interface is around hundred nm,[8] where it is difficult to analyze biomolecules and their spatial distribution at the interface in detail.

Scanning transmission X-ray microscopy (STXM)-based near-edge X-ray absorption fine structure (NEXAFS) with a soft X-ray region is a new tool applicable to the direct analysis of hydrated organic materials. The STXM-based NEXAFS has multiple advantages such as the ability of soft X-rays to penetrate water, presence of suitable analytical absorption edges (e.g., carbon, oxygen, and nitrogen) in the soft X-ray region, and low radiation damage compared to that of an electron beam technique like transmission electron microscopy (TEM).[9] The STXM also provides a high spatial resolution of better than 50 nm. Thus, the STXM-based NEXAFS allows us to obtain quantitative chemical speciation and spatial distribution of major biomolecules at the single-cell level even in samples composed of various constituents.

The objective of this study was to apply the STXM technique into bioleaching samples containing multiple constituents (microbes, minerals, and biomolecules) and investigate the efficiency of the STXM technique to identify in situ biological organic matters and its spatial distribution.

Bioleaching experiments were performed in batch cultures with 5 wt % pyrite in 10 mL of basal salt solution at 30 °C.[10] Powdered natural pyrite (Navajún mine, Spain; particle size 50–100 μm) and acidophilic chemoautotrophic Fe(II)-oxidizing bacteria *Acidithiobacillus ferrooxidans* ATCC 23270 were used as the metal sulfide and bioleaching microbe, respectively. *A. ferrooxidans* is one of the most important bacterial species of bioleaching microbes.[11] Suspension samples for the following analyses were collected after 30 days incubation, a gentle log phase in the growth curve. For STXM analysis, a small amount of collected suspension was dropped on a Si_3N_4 membrane and air-dried at room temperature. The STXM analyses for oxygen (O) and carbon (C) 1s NEXAFS were performed on two STXM apparatuses newly installed in BL-4U at UVSOR (Okazaki)[12] and BL-13A at KEK-PF (Tsukuba)[13] in Japan. The theoretical, spatial, and spectral resolutions of the STXM were less than 50 nm and ±0.1 eV. STXM measurements were performed at RT and at ca. 1/6 atm He. All STXM data processing was carried out using the IDL package aXis 2000.[14]

Figure 1 shows the STXM-based O1s NEXAFS of *A. ferrooxidans* cells attached on the pyrite particle and model compounds. For O and C NEXAFS, sodium alginate (acidic polysaccharide), agarose (neutral polysaccharide), albumin (protein), *Escherichia coli* DNA (nucleic acid), and 1,2-dipalmitoyl-*sn*-glycero-3-phosphoethanolamine (lipid) were selected as model compounds following previous studies.[2,5] In these model compounds, a sharp first peak was similarly observed at 532 eV, and a broad second peak was observed at a range of 535–550 eV. Due to these overlapping signals, our O NEXAFS spectra cannot conclusively determine whether the organic O in the *A. ferrooxidans* is derived from sugars, lipids, and proteins. However, the O NEXAFS spectra for bacterial cells show significantly similar spectral features as those observed for O in protein and polysaccharide.

STXM-based C image and NEXAFS spectra are shown in Figure 2. The center of the image shows a pyrite particle,

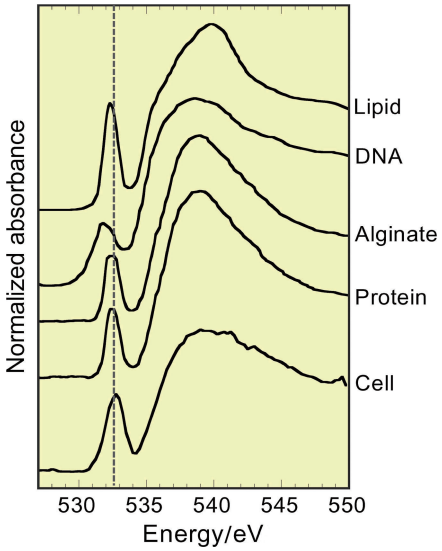

Figure 1. STXM-based O1s NEXAFS spectra of model compounds and *A. ferrooxidans* cell on pyrite grain (30 days incubation). A dotted line stands for 1st peaktop energy of bacterial cell.

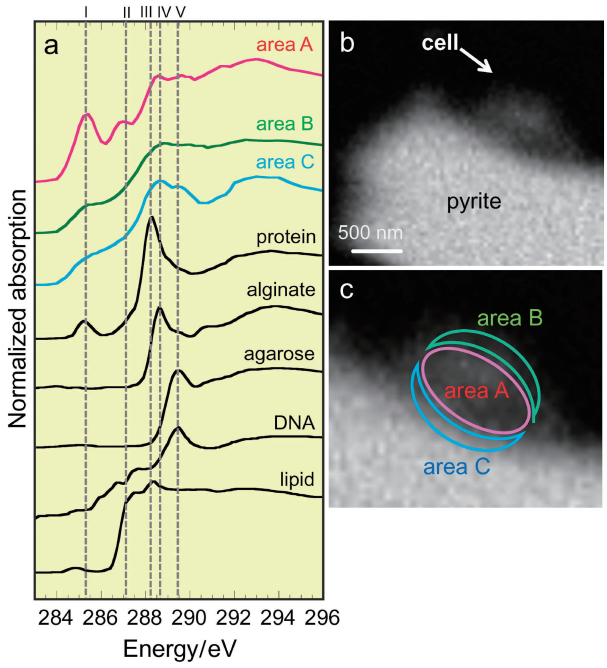

Figure 2. STXM-based C1s NEXAFS and image of model compounds and *A. ferrooxidans* cell on the pyrite grain (30 days incubation). Absorption edge peaks are identified as aromatic C at 285.2 eV (I), aliphatic C at 287.3 eV (II), amide C at 288.2 eV (III), carboxylic C at 288.6 eV (IV), and O–alkyl C at 289.4 eV (V).

because the X-ray absorption of this area is saturated with an optical density of more than 2 (Figure 2b). In C1s NEXAFS, in Figure 2a, the spectral features of the model compounds showed a clear difference in each compound for polysaccharide, lipid, protein, and nucleic acid (functional group and transition

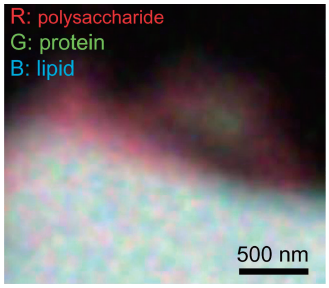

Figure 3. Color-coded compositional image. Images collected at each specific absorption edge (polysaccharide: 288.6 eV, protein: 288.2 eV, and lipid: 287.3 eV) were merged in the image.

corresponding to each peak are summarized in Table S1 in Supporting Information (SI)). Hence, we used C NEXAFS to identify biogenic molecules. The spectrum of pyrite-attached *A. ferrooxidans* cell (area A) consisted of peaks representing aromatic (I), aliphatic (II), amide (III), carboxy (IV), and O–alkyl (V) C (Figure 2a). Basically, the spectral feature was similar to a mixture of albumin, alginate, and lipid exhibiting major peaks of aromatic at 285.2 eV (I), aliphatic at 287.3 eV (II), amide at 288.2 eV (III), and carboxy 288.6 at eV (IV), which is agreeable with O NEXAFS. On the other hand, a significant difference was found in the spectra of the rim of the cell (area B) and cell–pyrite boundary (area C). The spectra of areas B and C mainly consist of carboxy, typical for acidic polysaccharides like alginate, whereas aromatic (I), aliphatic (II), and amide (III) peaks largely diminished compared with the whole cell (area A). These findings imply that *A. ferrooxidans* produces polysaccharide-rich biomolecules at the cell–pyrite interface. The nanoscale color-coded compositional map (red: polysaccharide, green: protein, and blue: lipid) in Figure 3 shows the spatial distribution of these biomolecules. The polysaccharide was abundant in the rim of the cell (pyrite–cell boundary) and pyrite surface, while the protein- and lipid-rich regions were in the center region of the cell, which is consistent with C NEXAFS spectroscopy. The thickness of the polysaccharide-rich layer is around 100–150 nm. Thus, the findings consistently suggest that the polysaccharide abundant layer is localized in the cell–pyrite boundary and that *A. ferrooxidans* produces EPS abundant in polysaccharide at the cell–pyrite interface, which is also supported by fluorescence staining with a polysaccharide-specific dye (Figure S1 in SI).

There are many previous studies on the biofilm formation and EPS components of *A. ferrooxidans* in the bioleaching process.[5,11,15,16] They reported that *A. ferrooxidans* grown in the pyrite medium produces EPS including various biopolymers such as proteins, polysaccharides, lipids, and nucleic acids. However, these studies are based on destructive bulk analyses of the exopolymeric matrix extracted from a mixture of planktonic and sessile cells, which limits critical information on spatial distribution and the structure of these constituents, and this type of information is highly relevant to understanding the bioleaching process at the cell–mineral interface. Our direct analysis by STXM clearly showed that a polysaccharides-abundant EPS was produced on the pyrite by *A. ferrooxidans* and was localized at the cell–pyrite boundary within 150 nm. *A. ferrooxidans* may use the polysaccharides to enhance pyrite dissolution, because

polysaccharides produced by *A. ferrooxidans* form Fe(II) complexes and mediate subsequent oxidation attack.[11]

There are very few applications of the STXM technique into in situ monitoring of extracellular polymer substance of bioleaching bacteria. The STXM has multiple advantages: (i) a high spatial resolution below 50 nm is sufficient to analyze local reaction field in microbe–mineral interface; (ii) a nondestructive analysis is useful to investigate spatial distribution of biomolecules with high elemental specificity; (iii) X-ray spectroscopic speciation with an He purge is functional to analyze hydrated biomolecules with minimum damage compared with the electron beam technique. Thus, STXM-based NEXAFS technique would be a powerful tool for investigating mechanisms of biological process occurring at the microbe–mineral interface.

The synchrotron experiments were performed with the approval of KEK (Proposal Nos. 2013S2-003 and 2012G640) and UVSOR (Proposal No. S-13-MS-1005).

Supporting Information is available electronically on J-STAGE.

References

1 H. Tributsch, *Hydrometallurgy* **2001**, *59*, 177.
2 G. J. Olson, J. A. Brierley, C. L. Brierley, *Appl. Microbiol. Biotechnol.* **2003**, *63*, 249.
3 G. J. Olson, *Appl. Environ. Microbiol.* **1991**, *57*, 642.
4 X. Lu, H. Wang, *Elements* **2012**, *8*, 119.
5 B. Vu, M. Chen, R. J. Crawford, E. P. Ivanova, *Molecules* **2009**, *14*, 2535.
6 S. Bellenberg, C.-F. Leon-Morales, W. Sand, M. Vera, *Hydrometallurgy* **2012**, *129–130*, 82.
7 T. Rohwerder, T. Gehrke, K. Kinzler, W. Sand, *Appl. Microbiol. Biotechnol.* **2003**, *63*, 239.
8 S. Mangold, M. Laxander, K. Harneit, T. Rohwerder, G. Claus, W. Sand, *Hydrometallurgy* **2008**, *94*, 127.
9 K. Tsuji, K. Nakano, Y. Takahashi, K. Hayashi, C.-U. Ro, *Anal. Chem.* **2010**, *82*, 4950.
10 M. E. Mackintosh, *Microbiology* **1978**, *105*, 215.
11 T. Gehrke, J. Telegdi, D. Thierry, W. Sand, *Appl. Environ. Microbiol.* **1998**, *64*, 2743.
12 T. Ohigashi, H. Arai, T. Araki, N. Kondo, E. Shigemasa, A. Ito, N. Kosugi, M. Katoh, *J. Phys.: Conf. Ser.* **2013**, *463*, 012006.
13 Y. Takeichi, N. Inami, H. Suga, K. Ono, Y. Takahashi, *Chem. Lett.* **2014**, *43*, 373.
14 A. P. Hitchcock, **2009** (http://unicorn.mcmaster.ca/aXis2000.html).
15 H. C. Flemming, J. Wingender, *Nat. Rev. Microbiol.* **2010**, *8*, 623.
16 J. Hao, R. Murphy, E. Lim, M. A. A. Schoonen, D. R. Strongin, *Geochim. Cosmochim. Acta* **2009**, *73*, 4111.

